Assessment of the Antenna-Equivalence Approach to Common-Mode Input Impedance Modeling

Assessment of the Antenna-Equivalence Approach to Common-Mode Input Impedance Modeling

A. Hubrechsen[1], L. A. Bronckers[1] and A. Roc'h[1]

[1] Eindhoven University of Technology, Department of Electrical Engineering, Eindhoven, The Netherlands

***Abstract*—Analytical modeling of the common-mode input impedance of a motor along with its cable for various installation characteristics would allow designers to assess EMI levels and to evaluate in an early stage if adaptations are needed in their cable installation. Earlier work has shown that the input impedance over frequency of such a system is mostly dominated by the cable. A common assumption is that a cable can be approximated as a monopole antenna above a ground plane, which has an input impedance equivalent to that of a dipole with a correction factor. We compare the *Hallén* and *King & Middleton* dipole models to a measurement setup which is designed to reproduce parastic effects from the installation, to assess the validity of the analytical model. We analyze these results for various distances between the cable and the groundplane. We show that large discrepancies occur due to paristics of the installation and the presence of the groundplane, but that for some applications such closed-form analytical models may suffice in assessing frequencies at which radiated emissions occur.**

***Index Terms*—Antenna, Common-mode, EMC, EMI, Hallén, Impedance, King and Middleton, Model, Thin-wire theory**

I. Introduction

Common-mode currents (or asymmetric currents) are known to be the principal contributor of radiated emissions in installations [1], potentially causing electromagnetic interference (EMI) in a system. Especially in motor-drive systems, it is critical to asses these levels in order to take appropriate measures, for example by means of common-mode chokes, shielding, or an output EMI filter [2], [3]. Most modeling techniques used to asses EMI levels are generally time-consuming and expensive. Therefore, there is a need for characterizing the level of EMI by use of analytical methods.

Earlier work has shown that the common-mode impedance in a motor-drive system is dominated by its cable impedance [4]. Therefore, radiated emissions of a motor-driven system may be analyzed by assessing the behavior of the cable. Typically, interference effects in cables are modeled using multiconductor transmission line (MTL) theory [5]–[7]. This analytical approach is widely used, but it has shown to be unsuitable to characterize radiated emissions due to their assumption on the transverse-electromagnetic mode [7]. MTL theory has been extended to assess field-to-wire coupling by incorporating the tangential and parallel components of the electric and magnetic fields of an incident plane wave as induced voltages and currents in the TL, respectively [8]. However, this can lead to significant inaccuracies since, in practice, a cable-bundle generally resides in a scattering environment [9], [10]. Other techniques use full-wave simulations such as method-of-moments or finite-difference-time-domain techniques to assess radiated emissions [11], [12], but these are often too time-costly and complex to be used by engineers, especially when a quick decision is needed to make an adaptation.

Another technique that is rarely referred to in power-electronics applications is to model the cable as an antenna. Especially for higher frequencies and for cable heights above the groundplane greater than a tenth of the wavelength, the antenna behavior of a cable starts to dominate [13]. Some research has been performed on modeling a cable above a ground plane as an antenna by use of thin-wire theory [4], [12], which used the assumption that a cable acts as a monopole antenna above a ground plane [12], [14]–[16]. However, these models still use time-costly full-wave techniques, or they assumed setups that are different from reality [12].

In this work, we introduce a new measurement setup that is closer to reality by taking the proximity of the installation into account and, for the first time, we compare its behavior to an analytical model of a monopole antenna above a groundplane up to 1 GHz. We present an analysis of the effects of increasing the cable height, and discuss the possible effects of the proximity of the installation on the common-mode input impedance. Using these results, we also analyze the validity of approximating such a setup as a monopole above a groundplane. In Section II, we present the measurement setup, and the analytical antenna model used to compare the results with, which we discuss in Section III. In Section IV we discuss effects that were not taken into account in this measurement setup. The work is concluded in Section V.

II. Antenna Equivalence

In this section, we provide a measurement setup designed to replicate the conditions of a realistic installation, and we describe the methods used to measure and model the common-mode input impedance, which can be used to asses frequencies at which EMI levels can become significant.

A. Experiment Design

To accurately model the common-mode input impedance, the setup was chosen to be an accurate representation of reality. We represent a motor-drive system with a cable attached to it,

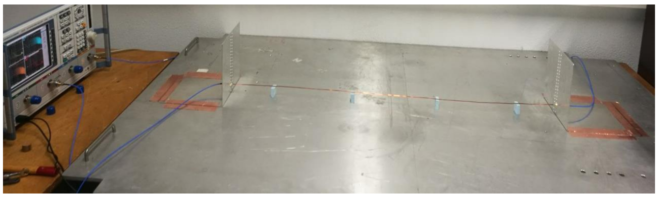

Fig. 1. The measurement setup.

TABLE I
VNA SETTINGS

VNA Setting	Value
Stimulus power	5 dBm
Frequency band	10 MHz - 1 GHz
Frequency points	1301
IF BW	100 Hz
Calibration type	Short-Open-Load-Thru
Calibration kit	Mechanical 3.5mm precision kit

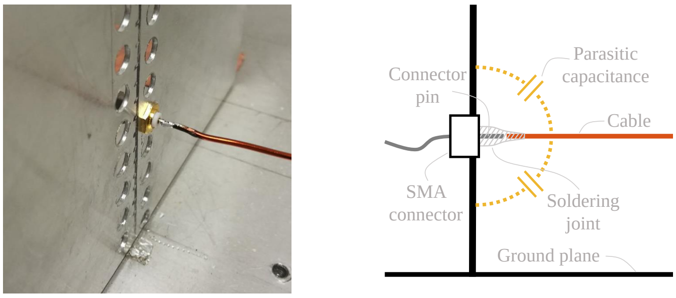

(a) (b)

Fig. 2. The connection at the vertical metal plate in the measurement setup (a) and as an illustration (b). The parasitic capacitances between the cable and the plate can affect the measured input impedance significantly.

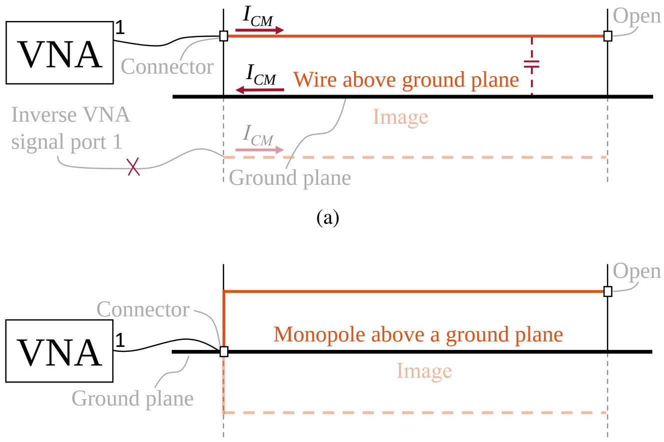

(b)

Fig. 3. An illustration of the setup to mimic a motor-drive system (a) and a commonly used way of modeling such a setup (b).

similar to [4], [12]. In [12], a cable was placed orthogonal to the ground plane. However, having the cable parallel to the ground, as was done in [4], is closer to real life. Therefore, we use a setup with a large ground plane to represent the ground, with two metallic plates attached to it with a thin wire in between them, since the motor exterior is metallic, and a three-phase cable may be represented as a thin wire [4]. This also allows us to assess the effect of the connection between the cable and the plate. The setup is shown in Fig. 1, where the holes in the metallic plates provide the option to measure at various heights. Common-mode impedance was measured by use of a vector network analyzer (VNA) connected to port 1, as these have the quality to measure impedance below 50 Ω, unlike the measurements performed in [4]. From such a measurement, the input impedance including parasitic effects between the cable and the vertical metallic plates can be determined, which is not possible in a measurement using a current probe, as a probe is used after the input. This effect is illustrated in Fig. 2. The VNA settings are shown in Table I. The cable is connected with an SMA connector, which is a good representation for common-mode propagation, due to a separation between the signal path and the ground return path. The cable was terminated in an open for modeling purposes and to obtain a general expression as a first step.

B. Antenna Modeling

The thin wire is often modeled as a monopole above a ground plane, as shown in Fig. 3(b). While the measurement setup is fundamentally different from a monopole above a groundplane, or a dipole, it is common practice to model it as such [4], [12], [14]–[16]. Due to image theory, it may also be modeled as a dipole, but if corrected for the fact that the input impedance of a monopole of length h equals half the input impedance of a dipole of length $2h$ [17]. This also covers the fact that a monopole resonates first at $\lambda/4$ and a dipole at $\lambda/2$. We used two analytical models to approximate the dipole, the first one being the *King & Middleton* approach, and the second one being the *Hallén* approach, where we take the correction into account. Both methods base the calculation of the input impedance on a mathematical expression of the current distribution along the antenna, where the exact expression is approximated by a sum of i^{th}-order impedances $(i = 0, 1, ...N)$ [18].

1) King & Middleton: The King & Middleton iterative solutions' initial approximation is based on the assumption that the vector potential is proportional to the current. This may not be valid at the ends of the dipole antenna, where rapid current changes occur, hence affecting the modeled impedance at the resonance frequencies [19]. This approach also assumes there are no ohmic losses in the antenna. The first-order solution of the King & Middleton solution is expressed as follows

$$\begin{aligned} Z =& 60\Psi * \left| \frac{a_1 + jb_1}{c_1 + jd_1} \right| \\ & * \exp\left[j\left(\tan^{-1}\left(\frac{b_1}{a_1}\right) - \tan^{-1}\left(\frac{d_1}{c_1}\right)\right)\right], \end{aligned} \tag{1}$$

TABLE II
LIST OF VARIABLES

Variable	Meaning	Value	Unit
a	Radius conductor	$1.7 \cdot 10^{-3}$	m
β_0	Wave number	$\frac{2\pi}{\lambda}$	m^{-1}
ζ_0	Free space wave impedance	376.73	Ω
λ	Wavelength	-	m
l	Length of the cable	1	m
μ	Absolute permeability	$1.257 \cdot 10^{-6}$	$H \cdot m^{-1}$
σ	Conductivity of the wire	$5.96 \cdot 10^{7}$	$S \cdot m^{-1}$
ω	Angular frequency	$2\pi f$	s^{-1}

where a_1, b_1, c_1, and d_1 can be found in [18], p.151, and where

$$\Psi = 2 * \ln\left(\frac{2l}{a}\right), \tag{2}$$

where l and a are defined in Table II. The full derivation can be found in [18].

2) Hallén: Hallén's solution is a zeroth-order solution frequently given in the literature. In this solution, the current along the antenna is assumed to be sinusoidal, and unlike the King & Middleton solution, this solution takes ohmic losses of the antenna into account. The input impedance is calculated using $Z = R_0 + X_0$, where R_0 and X_0 are given by

$$\begin{aligned} R_0 &= R_0^e + R_0^i, \\ X_0 &= X_0^e + X_0^i, \end{aligned} \tag{3}$$

where R^i is an internal resistances due to dissipation in the conductor and R^e an external resistance due to radiation. It should be noted that these resistances are assumed to be independent in the zeroth order. For higher orders the distribution of the current becomes more complex and is determined by radiation and thermal dissipation. In practice, this effect is not significant when good conductors are used because internal resistance due to dissipation may be neglected. The definitions of the variables in (3) are given by

$$\begin{aligned} R_0^e =& \frac{\zeta_0}{4\pi} * \Bigg[\Big(1 - \cot^2(\beta_0 h)\Big) * \mathrm{Cin}(4\beta_0 h) \\ &+ 4\cot^2(\beta_0 h) * \mathrm{Cin}(2\beta_0 h) \\ &+ 2\cot(\beta_0 h) * \Big(\mathrm{Si}(4\beta_0 h) - 2\mathrm{Si}(2\beta_0 h)\Big)\Bigg], \end{aligned} \tag{4a}$$

$$\begin{aligned} X_0^e =& \frac{\zeta_0}{4\pi} * \Bigg[\Big(1 - \cot^2(\beta_0 h)\Big) * \mathrm{Si}(4\beta_0 h) \\ &+ 4\cot^2(\beta_0 h) * \mathrm{Si}(2\beta_0 h) \\ &+ 2\cot(\beta_0 h) * \Big(2\mathrm{Cin}(2\beta_0 h) \\ &- \mathrm{Cin}(4\beta_0 h) - 2\ln(\frac{h}{a})\Big)\Bigg], \end{aligned} \tag{4b}$$

$$\begin{aligned} R_0^i =& X_0^i = \frac{1}{2\pi a \beta_0}\sqrt{\frac{\omega\mu}{2\sigma}} \\ &* \Big[\beta_0 h * \csc^2(\beta_0 h) - \cot(\beta_0 h)\Big], \end{aligned} \tag{4c}$$

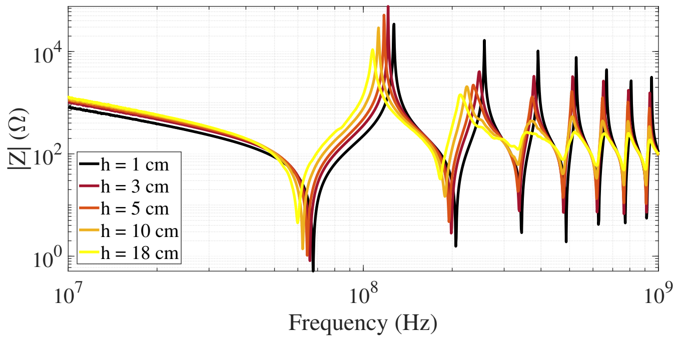

Fig. 4. Measured input impedance for various heights.

where the definitions of β_0, ζ_0, μ, ω and σ are given in Table II. The full derivation can be found in [18], p. 147.

III. RESULTS

In this section, we discuss the measured results, and compare them to the *Hallén* and *King & Middleton* analytical models.

A. Measurement results evaluation

Fig. 4 shows the common mode input impedance over a frequency, measured using the setup in Fig. 1 which was terminated in an open. We expect that all resonances (shown by the peaks and nulls in Fig. 4) can be attributed to radiated emissions, as they correspond to the wavelengths at which standing waves occur in the cable. Multiple effects can be observed when the height is increased.

First, we focus on the response before the first resonance (below 50 MHz), where the impedance is solely capacitive. If the height is increased, the capacitive behavior reduces. We expect that this can be attributed to less coupling with the groundplane, reducing parasitic capacitances. Second, we focus on the effects that occur in frequencies higher than 50 MHz. A clear shift can be observed from the resonances to lower frequencies. We expect this effect occurs due to the prominent effect of the groundplane in the reactive near field of the antenna for (electrically) small separations between the cable and the groundplane. This implies that the shift is larger for lower frequencies, which we will show in comparison to the modeled results. Lastly, increasing the height reduces the maximum and minimum measured impedance values, and 'widens' the response of each resonance over frequency, implying higher resistive losses. We expect that these are mainly radiation losses, as antenna behavior becomes more prominent at greater heights [13].

B. Modeled Results

Fig. 5 shows the modeled results using the *Hallén* and *King & Middleton* methods, compared to the measured result at h = 1 cm. Clear differences in magnitude can be observed, since the presence of the groundplane and the vertical metal plates may introduce capacitive behavior that shifts the measured results to lower magnitude and to lower frequencies. Note that

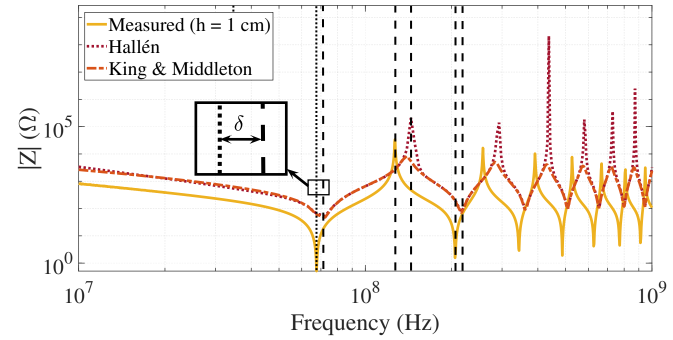

Fig. 5. The modeled and measured results. The magnitudes differ significantly, showing that the dipole-equivalence approach is not sufficient to assess EMI levels.

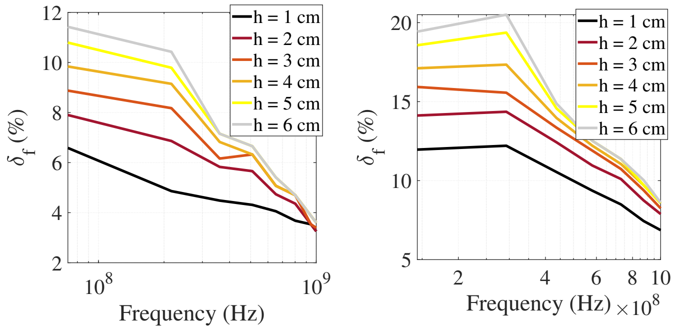

(a) (b)

Fig. 6. The discrepancy of the measured resonance frequency to the simulated one for all minimum (a) and maximum resonances (b), measured at different heights and normalized to the modeled resonance frequency.

this capacitive effect is possibly less significant in the modeled results, since the analytical models do not take into account that the cable is close to the groundplane for the complete length of the cable. The possible shift due to this assumption can be observed in Fig. 6, where we calculated the difference between the minimum and maximum measured and modeled impedance at each resonance frequency, normalized to the modeled resonance frequency. For the sake of clarity, we only show heights up until 6 cm, since the discrepancy surpasses 50 % after that. The figure shows that the difference becomes smaller (approximately 2-7 % absolute for the resonances at minimum impedance and approximately 5-11 % for those at maximum impedance) for higher frequencies, implying that the effect occurs due to the more prominent presence of the groundplane at cable heights that are small compared to the wavelength.

IV. Discussion

As we have shown, the presence of the groundplane has a significant effect on the measured common-mode input impedance, causing significant differences with a modeled dipole. While it is often expected that they produce similar results, these structures are fundamentally different since the model does not take into account that the full length of the cable is close to the groundplane. Therefore, that configuration puts the assumption that a cable above a groundplane is equivalent to a monopole above a groundplane at the edge of its validity. On the other hand, while the presence of the groundplane in the reactive nearfield causes large discrepancies in terms of magnitude, the shift in resonance frequency may be acceptable for some applications, as they reduce for higher frequencies and lower heights.

V. Conclusion

In this work, we have analyzed the use of analytical models to approximate radiated emissions in a cable in a motor-drive system as a dipole or a monopole above a groundplane, as is common practice in EMC. We introduced a more realistic setup which takes installation effects of the motor into account and allows for measuring various heights. We compared the results obtained by this setup to the analytical *Hallén* and *King & Middleton* models of a dipole. We found that large discrepancies occur between the modeled and measured results. We expect that these can be attributed to additional capacitive effects introduced by the installation and by the presence of the groundplane over the entire length of the cable in the setup, while both these effects are not taken into account in the model. This puts the dipole-equivalence, or monopole-above-a-groundplane equivalence, assumption at the edge of its validity. However, depending on the application, discrepancies due to usage of a dipole analytical model may be acceptable as using such a model is less complex and takes much less simulation time as compared to full-wave modeling. A more extensive analysis on the radiated emissions of this setup will be covered in future publications.

References

[1] C. R. Paul, “A comparison of the contributions of common-mode and differential-mode currents in radiated emissions,” *IEEE Transactions on Electromagnetic Compatibility*, vol. 31, no. 2, pp. 189–193, May 1989.

[2] G. L. Skibinski, R. J. Kerkman, and D. Schlegel, “EMI emissions of modern PWM AC drives,” *IEEE Industry Applications Magazine*, vol. 5, no. 6, pp. 47–80, Nov 1999.

[3] A. Roc’h and F. Leferink, “In situ performances of common mode chokes,” in *10th International Symposium on Electromagnetic Compatibility*, Sep. 2011, pp. 494–499.

[4] A. Roc’h and F. Leferink, “Experimental investigation of the input common mode impedance of a motor and its cable up to 1GHz,” in *2014 International Symposium on Electromagnetic Compatibility*, Sep. 2014, pp. 631–636.

[5] A. Vukicevic, F. Rachidi, M. Rubinstein, and S. V. Tkachenko, “On the evaluation of antenna-mode currents along transmission lines,” *IEEE Transactions on Electromagnetic Compatibility*, vol. 48, no. 4, pp. 693–700, Nov 2006.

[6] D. Poljak, A. Shoory, F. Rachidi, S. Antonijevic, and S. V. Tkachenko, “Time-domain generalized telegrapher’s equations for the electromagnetic field coupling to finite length wires above a lossy ground,” *IEEE Transactions on Electromagnetic Compatibility*, vol. 54, no. 1, pp. 218–224, Feb 2012.

[7] S. A. Pignari, “Deterministic and statistical emc models for field-to-wire coupling and crosstalk in wire harness,” in *Handbook of Aerospace Electromagnetic Compatibility*, 2019, pp. 79–119.

[8] C. R. Paul, “Frequency response of multiconductor transmission lines illuminated by an electromagnetic field,” *IEEE Transactions on Electromagnetic Compatibility*, vol. EMC-18, no. 4, pp. 183–190, 1976.

[9] D. Bellan and S. Pignari, “A probabilistic model for the response of an electrically short two-conductor transmission line driven by a random plane wave field,” *IEEE Transactions on Electromagnetic Compatibility*, vol. 43, no. 2, pp. 130–139, 2001.
[10] M. Magdowski and R. Vick, “Closed-form formulas for the stochastic electromagnetic field coupling to a transmission line with arbitrary loads,” *IEEE Transactions on Electromagnetic Compatibility*, vol. 54, no. 5, pp. 1147–1152, 2012.
[11] D. M. Hockanson, J. L. Drewniak, T. H. Hubing, and T. P. Van Doren, “Fdtd modeling of common-mode radiation from cables,” *IEEE Transactions on Electromagnetic Compatibility*, vol. 38, no. 3, pp. 376–387, 1996.
[12] R. Mestrom, A. Roc’h, and Y. Xi, “Modeling the common mode impedance of motor drive systems using the antenna wire concept,” in *2015 IEEE International Symposium on Electromagnetic Compatibility (EMC)*, Aug 2015, pp. 1412–1415.
[13] G. Andrieu, L. KonÉ, F. Bocquet, B. DÉmoulin, and J. Parmantier, “Multiconductor reduction technique for modeling common-mode currents on cable bundles at high frequency for automotive applications,” *IEEE Transactions on Electromagnetic Compatibility*, vol. 50, no. 1, pp. 175–184, 2008.
[14] K. Fukuzawa, M. Tada, T. Yoshikawa, K. Ouchi, and R. Sato, “A new method of calculating 3-meter site attenuation,” *IEEE Transactions on Electromagnetic Compatibility*, vol. EMC-24, no. 4, pp. 389–397, 1982.
[15] A. T. Adams, J. Perini, M. Miyabayashi, D. H. Shau, and K. Heidary, “Electromagnetic field-to-wire coupling in the shf frequency range and beyond,” *IEEE Transactions on Electromagnetic Compatibility*, vol. EMC-29, no. 2, pp. 126–131, 1987.
[16] B. van Leersum, J. van der Ven, H. Bergsma, F. Buesink, and F. Leferink, “Protection against common mode currents on cables exposed to hirf or nemp,” *IEEE Transactions on Electromagnetic Compatibility*, vol. 58, no. 4, pp. 1297–1305, 2016.
[17] M. M. Weiner, *Monopole Antennas*. New York: Marcel Dekker, Inc., 2003.
[18] R. W. P. King, *The Theory of Linear Antennas*, 1956.
[19] T. T. Wu, “Technical report on the theory of the dipole antenna and the two-wire transmission line,” *Technical Report No. 318, Office of Naval Research*, Mar. 1960.